



The plasma levitation of droplets

Cédric Poulain, Antoine Dugué, Antoine Durieux, Nader Sadeghi, and Jérôme Duplat

Citation: *Applied Physics Letters* **107**, 064101 (2015); doi: 10.1063/1.4926964

View online: <http://dx.doi.org/10.1063/1.4926964>

View Table of Contents: <http://scitation.aip.org/content/aip/journal/apl/107/6?ver=pdfcov>

Published by the [AIP Publishing](#)

Articles you may be interested in

[Heat flux modeling using ion drift effects in DIII-D H-mode plasmas with resonant magnetic perturbations](#)

Phys. Plasmas **21**, 012509 (2014); 10.1063/1.4862034

[Understanding the bursty electron cyclotron emission during a sawtooth crash in the HT-7 tokamak](#)

Phys. Plasmas **21**, 012501 (2014); 10.1063/1.4861336

[Shape oscillations of an electrically charged diamagnetically levitated droplet](#)

Appl. Phys. Lett. **100**, 114106 (2012); 10.1063/1.3694055

[The influence of temporal phase difference of \$m = \pm 2\$ oscillations on surface frequency analysis for levitated droplets](#)

J. Appl. Phys. **106**, 034907 (2009); 10.1063/1.3190495

[Levitation of positively charged fine particles in a cross-field sheath between magnetized double plasmas](#)

Phys. Plasmas **11**, L5 (2004); 10.1063/1.1649991

The logo for AIP Applied Photonics (APL Photonics) is displayed in a white font on a red background. The letters 'AIP' are large and bold, followed by a vertical bar and the words 'APL Photonics' in a smaller font.

AIP | APL Photonics

APL Photonics is pleased to announce
Benjamin Eggleton as its Editor-in-Chief



The plasma levitation of droplets

Cédric Poulain,^{1,a)} Antoine Dugué,² Antoine Durieux,² Nader Sadeghi,³ and Jérôme Duplat⁴

¹CEA, LETI, F38054, Grenoble, France

²Ecole Polytechnique, Palaiseau, France

³Univ. Grenoble Alpes & CNRS (UMR5588), LIPhy, Grenoble, France

⁴Univ. Grenoble Alpes, INAC SBT, Grenoble, France

(Received 2 June 2015; accepted 4 July 2015; published online 11 August 2015)

We show how to levitate a liquid droplet above a plasma. Submitting a conductive droplet to a voltage larger than 50 V, we get a levitation regime that looks like the one obtained with the well-known thermal Leidenfrost effect, except that light is emitted from beneath the droplet. Spectroscopic analysis shows that this light is emitted by a cold and dense plasma and also that lines coming from the cathode plate material are present revealing a local cathodic sputtering effect. We examine the conditions for the levitation to occur and show that the levitation is essentially of thermal origin. Assuming a stationary heat transfer, we present a model that accounts well for the observed levitation conditions. In particular, stable levitation is shown to be possible for thin cathode plates only. © 2015 AIP Publishing LLC. [<http://dx.doi.org/10.1063/1.4926964>]

It is well known that when a droplet is deposited on a sufficiently hot plate it can levitate above the plate. This levitation requires a plate temperature above the so-called Leidenfrost temperature, which is typically 280 °C for a water droplet.¹ The mechanism is quite well understood: liquid vaporization at the droplet lower interface produces vapor that flows beneath the droplet, and induces a pressure elevation that lift up the droplet.^{2,3} This calefaction phenomenon, also referred as Leidenfrost effect, has been extensively studied (see Ref. 1 for a review) More recently, original examples have been published in which a magnetic effect⁴ or electric effect⁵ have been added on top of the calefaction process to control and act upon the levitation.

Here, we report on the possibility to achieve levitation of millimetric water droplets by applying a voltage above 50 V on it with a mean current of 50 mA, over *thin conductive* plates. Indeed, as soon as the electric current crosses the droplet, electric arcs between the droplet lower interface and the metallic plate are formed, leading to cathodic sputtering and the formation of a cold plasma. The arcs region is surrounded by a vapor layer which is formed because of the Joule dissipation mainly localized in this gap, which in turn ensures a sufficient steam flow to maintain levitation. Finally, we will show that increasing the thickness of the plate lowers the surface temperature and hence yields to the wetting of the drop by promoting condensation of the steam.

The experimental configuration is shown in Fig. 1. A conductive droplet (2.0 mol l^{-1} HCl aqueous solution) is pinned at the tip of a stainless steel needle (inner diameter: 1.3 mm) and fed by a syringe pump. Initially, the needle is located $l = 4 \text{ mm}$ above a metallic plate (stainless steel or copper) of thickness $h = 0.1 \text{ mm}$, 1 mm, or 10 mm.

By means of a high-speed stabilized voltage generator, we impose a positive potential drop between the needle (anode) and the plate (cathode). The actual voltage U and current I through the droplet are recorded thanks to a 4-wire measurement device.

The general protocol is the following: First, a droplet is produced and suspended at the tip of the anode. Then, a voltage difference U is imposed between the needle and the cathode plate. No current flows since the drop is too far from the cathode (open circuit). Finally, the droplet is moved down closer to the bottom plate until electrical contact is triggered. For low voltage ($U < 50 \text{ V}$), the droplet wets the plate as soon as it touches it, so that it closes the electric circuit. Gas bubbles are produced at a high rate (foam like) with a current intensity of the order of 1 A, consequently the droplet vanishes quickly ($\sim 10 \text{ s}$, mainly by Joule heating) and no levitation is observed.

Restarting with another drop but increasing the voltage above 50 V yields to a severe increase of the droplet lifetime. In this regime, the current fluctuates around 50 mA and the phenomenon can last for a few minutes provided that the drop is continuously fed and also that the plate is thin enough. Moreover, blue light is emitted beneath the droplet

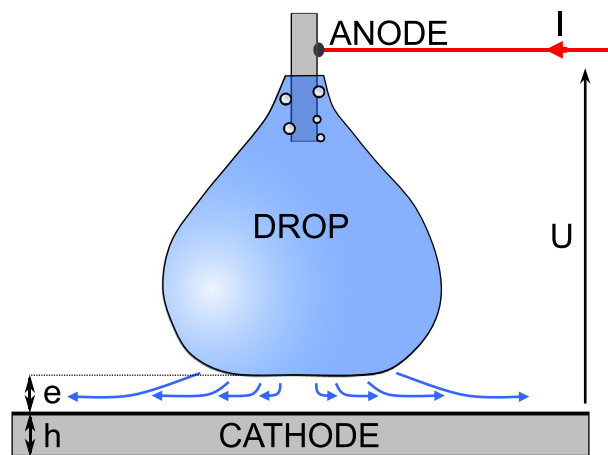


FIG. 1. Sketch of a typical electrolytic setup implemented for levitation. The electrolyte is a water-HCl droplet suspended to the tip of a needle. A metal plate is used as cathode. When the electric circuit is closed, oxygen is produced at the anode; while hydrogen is produced at the base of the drop. The plasma is localised in the vicinity of the lower interface.

^{a)}Electronic address: cedric.poulain@cea.fr

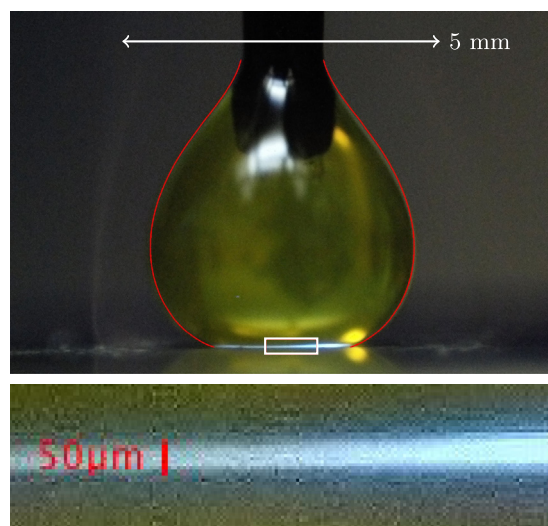


FIG. 2. Top: Color snapshot of a “levitating” droplet in the plasma regime. $U = 57.5$ V, $I \approx 50$ mA, aqueous HCl solution ($c = 2.0$ mol l^{-1}). The green color from the droplet comes from the chloride reduction ($2Cl^- \rightarrow Cl_2 + 2e^-$). The thin plasma layer beneath the droplet emits the blue light. Red curve: fit of the drop contour¹¹ yielding to geometric parameters for the model. Bottom: detail of the plasma region of thickness estimated as $e \approx 50$ μ m.

interface from a very thin layer (estimated from close snapshots to be of the order of $e \approx 50$ μ m, see Fig. 2). In the present study, water electrolysis produces H_2 vapor at the cathode, and O_2 vapor at the anode whose total mass-rate \dot{m}_{elec} is proportional to the electrical current I in the cell: $\dot{m}_{elec} = \frac{IM_{H_2O}}{2\mathcal{F}}$, where M_{H_2O} stands for the molar mass of water and \mathcal{F} is the Faraday’s constant.

To estimate the part of electrolysis in the drop lifetime, a dedicated experiment shown in Fig. 3 has been implemented with a non-fueled drop. The mean current is of the order of 50 mA. The corresponding electrolysis mass rate $\dot{m}_{elec} = 4.7 \times 10^{-9}$ kg s^{-1} is much smaller than the measured mass reduction rate for the non-fueled drop: $\dot{m}_{exp} \approx 3 \times 10^{-7}$ kg s^{-1} , suggesting clearly that the electrolytic process is not responsible for the observed vanishing rate.

Thermocouples (K type, 250 μ m in size) inserted into the levitating drop reveal that the internal temperature of the drop reaches $T_{sat} \approx 100^\circ C$ within a few seconds. Besides, long-term levitation is observed only for thinner cathode

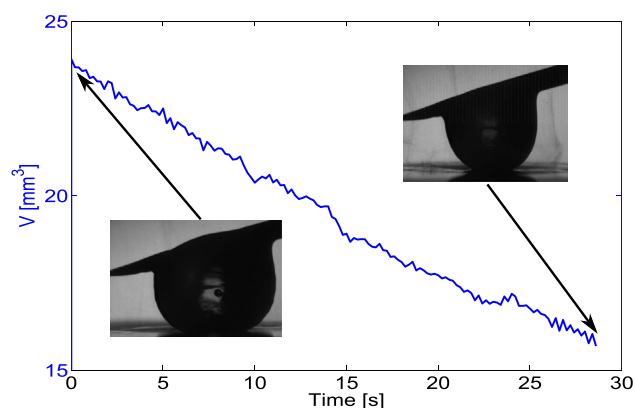


FIG. 3. Volume decrease as a function of time for a non-fueled drop (suspended to a metallic fiber) in the plasma levitation regime with 50 mA current. Volume is calculated from image processing.

plate ($h \leq 0.1$ mm), for which the plate temperatures lie between 100 and 150 $^\circ C$. For thicker plates, the levitation time is very short or even not possible for the 10 mm cathode. In both cases, the temperature of the plate remains below 100 $^\circ C$, suggesting a highly likely thermal origin of the observed levitation, as will be shown further.

Optical emission spectroscopy has been implemented to characterize the light emitted from the droplet base and in turn get more information on the nature of the plasma (composition, electron density). In order to control the influence of the surrounding atmosphere on plasma generation, the whole system has been enclosed in an air-tight chamber equipped with quartz viewports. Experiments were carried out with a chamber filled with either argon, helium, or nitrogen at $P \approx 1$ atm. The plasma layer between the drop and cathode was imaged on the entrance slit (100 μ m width) of a 1 m focal length monochromator (Jobin-Yvon, HR1000), equipped with a 1200 groves/mm grating. Spectra were acquired with a 1600 \times 400 pixel, 16 μ m pitch charge coupled device (CCD) camera. Regardless of the plasmogen gas used, the H_α line at 656.28 nm as well as the O triplet at 777 nm is always present in recorded spectra (see Fig. 4) but the H_β line at 486.13 nm could not be observed. Besides, with argon used as ambient gas, its 750.39 and 751.46 nm lines clearly show up in the recorded spectra. But none of the Helium and N lines, or of N_2 molecular bands are present in spectra recorded with these gases. Characteristic emission of OH radical around 300 nm and lines coming from the liquid (Cl or S in the case of using H_2SO_4 instead of hydrochloric acid) were also missing, whatever the surrounding gas. The absence of N_2 bands makes impossible to determine the gas temperature from the rotational structure of the band.⁶ Using Copper as cathode material, its resonance 324.75 and 327.40 nm lines as well as 510.55 and 578.21 nm lines are emitted by the plasma beneath the drop. In Fig. 4, the former two lines are seen in the second diffraction order of the grating. With stainless steel cathodes, many Iron, Chromium, and Nickel lines appear in the spectra revealing cathode sputtering by arcing phenomenon between the droplet and the cathode material.

As for the line shape, the Gaussian and Lorentzian parts of a profile are linked to the Doppler + instrumental widths

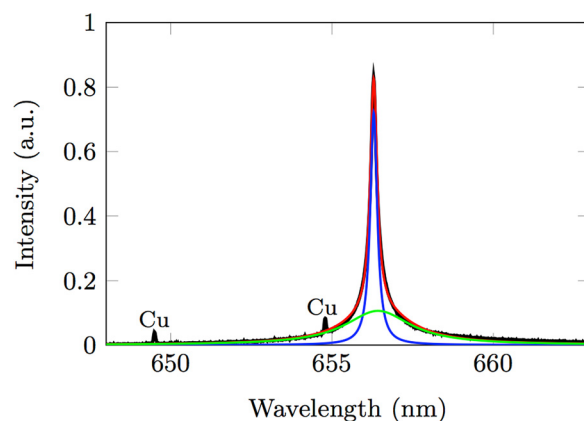


FIG. 4. Recorded profile of the H_α line under an helium atmosphere with copper cathode. The sum of two Lorentzians (blue and green) results in the red curve that fits the experimental data (black).

and pressure + Starks widths, respectively.⁷ In Fig. 4, the extended wings of the H_α line indicate that the pressure and/or Stark broadenings, who lead to Lorentzian profiles, are dominating the line shapes. Moreover, it is obvious that the profile cannot be reproduced with a single Lorentzian or Voigt profile and as shown in this figure the best fit is obtained by the sum of two Voigt, whose Full-Width at Half Maximum (FWHM) are $\Delta\lambda_m = 0.24$ and 2.57 nm, respectively.

These measured $\Delta\lambda_m$ of H_α line are much larger than the instrumental spectral width ($\Delta\lambda_i \approx 0.075$ nm at 656 nm), deduced from the width of Cu lines in Fig. 4. The Doppler width of H_α line (≈ 0.01 nm at $T_g = 400$ K (Ref. 6)) is much smaller than $\Delta\lambda_i$ and can be neglected. Also, applying the method described in Ref. 8, the pressure broadening in argon, the gas for which it is the most important, can be deduced from the relation $\Delta\lambda_p = 4.7/T^{0.7}$ nm, whose value at $T_g = 400$ K is $\Delta\lambda_p = 0.07$ nm. Applying relations given in Ref. 7 linking different widths, the deduced Stark widths of the narrow, and broad components of the profile presented in Fig. 4 are $\Delta\lambda_s = 0.13$ and 2.5 nm, respectively. Applying relation in Table 4 of Ref. 9, the estimated electron densities are $n_e = 3.9 \times 10^{21}$ and $4 \times 10^{23} \text{ m}^{-3}$ for the corresponding narrow and broad components of the H_α line in Fig. 4. It should be noted that these values vary from one cathode material or liquid to another and are only indicative of the orders of magnitude. The origin of two components in the H_α line is still unclear and probably stems from two distinct regions in the plasma layer or two plasma regimes.

Based on the above estimated electron density and nature of the plasma, we can now estimate the plasma conductivity and thereby present a simple model in good agreement with measurements made for the generic drop of Fig. 2 for different cathode thickness.

In the following, we will neglect both the drop electrical resistance (10Ω) which is negligible compared with the vapor layer resistance (and the chemical power needed for electrolysis which is less than 100 mW).

Thus, the total supplied electric power (of about 2.5 W) is dissipated on the one hand by Joule effect in the vapor film acting as a volume heat source of power \mathcal{P}_{Joule} , and by the ion bombardment \mathcal{P}_{Bomb} heating up the cathode surface on the other hand, so that $\mathcal{P}_{Elec} = \mathcal{P}_{Joule} + \mathcal{P}_{Bomb}$.

For a plasma of arcs of electrical resistivity ρ_p and thickness e , one can write: $\mathcal{P}_{Joule} = U^2 \epsilon S / \rho_p e$, where ϵ is a free parameter of the model and represents the cross-section of arcs compared with the total surface area S of the drop base. For plasmas of nature and densities comparable with the above measured one, we estimate $\rho_p \approx 10^{-3} \Omega \cdot \text{m}$.¹⁰ Fitting the drop contour with computed interface (using the method described in Ref. 11—see Fig. 2) that balances gravity against capillary force, it yields to an accurate measurement of geometrical properties of the drop (total volume, contact angle at the needle, and base area S).

The Joule power acts as a source term in the heat budget in the vapor thermal equilibrium. Introducing the Peclet number $Pe = \frac{\dot{m}_v e}{\rho_v S D}$, where \dot{m}_v , ρ_v , and D stand for the vapor mass rate, density, and thermal diffusivity, respectively, in

order to take the vertical vapor flow into account, and solving the heat equation averaged over time leads to vapor temperature profile $T_v(z)$ and consequently to the heat transferred to the drop \mathcal{P}_d , and to the cathode \mathcal{P}_c .¹² It yields to

$$\mathcal{P}_d = f_d(Pe) \mathcal{P}_{Joule} + g_d(Pe) \frac{k_v S}{e} (T_c - T_d), \quad (1)$$

with $f_d(Pe) \approx \exp(-\frac{Pe}{6})/2$. and $g_d(Pe) \approx \exp(-\frac{Pe}{3})$.

$$\mathcal{P}_c = f_c(Pe) \mathcal{P}_{Joule} - g_c(Pe) \frac{k_v S}{e} (T_c - T_d), \quad (2)$$

with $f_c(Pe) = \frac{1}{2} - \frac{Pe^2}{720} + o(Pe^2)$ and $g_c(Pe) \approx 1 + \frac{Pe}{6}$. At $z = 0$, the cathode is warmed up by ion bombardment and by the conductive transfer from the vapor layer. It acts like a cylindrical fin, so that the heat is spread radially prior to being transferred to the environment. The cathode temperature elevation can be estimated by

$$k_c h (T_c - T_0) \sim \mathcal{P}_c + \mathcal{P}_{bomb}, \quad (3)$$

where k_c and h are the cathode thermal conductivity and thickness and T_0 is the room temperature. At $z = e$ (droplet interface), conductive heat transfer to the drop forces evaporation at a rate $\dot{m}_v = \frac{\mathcal{P}_d}{L}$, with L the latent heat of water, yielding to the vapor layer thickness e .

Heat dissipated (due to Joule effect or ion bombardment) is transferred to the drop, to the environment, or to the vapor itself. The thermal resistance between cathode and the drop $e/[g_d(Pe)k_v S]$ is much larger than the thermal resistance between the cathode and the environment ($1/k_c h$) (in the least unfavorable case, i.e., $h = 100 \mu\text{m}$ one order of magnitude larger). Consequently, at most 10% of the heat supplied directly to the plate contributes to the evaporation process. This is an insufficient contribution and this cannot lead to levitation. On the contrary, dissipation in the vapor layer is in large proportion ($f_c(Pe)$) transferred to the drop. Hence, we will consider that the power is dissipated by Joule effect solely.

After numerical resolution with the parameters relevant to our experiment (U , S , k_v , ρ_e , k_c , h , T_0 , T_{sat}), the model leads to coherent values and tendencies consistent with observations (see Table I) for a specified cross section $\epsilon = 1/30\,000$. This value given by the model certainly indicates that the observed light results from a very large number of micro arcs, whose global area is approximately 4 orders of magnitude smaller than the base area.

The maximal temperature in vapor layer and the evaporation rate dependence on the plate thickness are extremely weak and could not justify that levitation is observed only

TABLE I. Comparison model/experiments for the drop of Fig. 2: $S = 4.3 \text{ mm}^2$ on a stainless plate ($h = 100 \mu\text{m}$). The free parameter $\epsilon = 1/30\,000$.

Quantity	Experiment	Model prediction
\dot{m}_v	$3 \times 10^{-7} \text{ kg/s}$	$4.7 \times 10^{-7} \text{ kg/s}$
e	$\sim 50 \mu\text{m}$	$130 \mu\text{m}$
T_c	$100\text{--}150^\circ\text{C}$	122°C

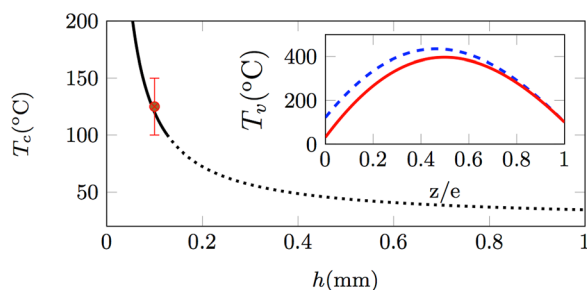


FIG. 5. Cathode temperature T_c as a function of the cathode thickness. Inset: predicted vertical temperature profile in the plasma region for $h = 100 \mu\text{m}$ (dashed blue) and $h = 1 \text{ mm}$ (continuous red) thickness plates. In this latter case, the predicted cathode temperature is 30°C , so that no levitation can be observed in this case. Calculations are made for $\epsilon = 1/30\,000$, the vapor layer thickness is found to be $\sim 130 \mu\text{m}$ in both cases.

for thin plates. Nonetheless, the cathode temperature decreases strongly with the plate thickness (see Fig. 5) and falls under 100°C for $h > 130 \mu\text{m}$. We believe that a hot cathode (i.e., $T_c > T_{\text{sat}}$) is a necessary condition for levitation to be maintained, otherwise the hot vapor will condense on the plate, electric contact will be recovered by the liquid bridge so that streamers and vapor production will cease, hindering levitation.

The low tension ($\sim 60 \text{ V}$) required for levitation is far below the minimum voltage ($\sim 320 \text{ V}$) given by Paschen law for the discharge breakdown between two electrodes.¹³ Here, the interesting point is that the anode is a liquid electrode likely to deform and destabilize. Liquid fingers may form and by Peek effect lower the minimum voltage for arcing. This scenario would also be compatible with the observation that levitation is observed and possible only for cathode temperature larger than the liquid saturation one (here about 100°), otherwise contact with the plate would cool the liquid and hence inhibit vaporisation and hinder levitation.

As we have shown, the drop levitates on a plasma composed of sparks arcing at the base of the drop acting as a hot source producing evaporation, and in turn ionizes the produced gases (essentially steam). A model has been presented and account for the observed vanishing rates, gap thickness, temperatures, and conditions for plasma levitation.

It is noteworthy that unlike the Leidenfrost levitation where drops can move freely on the hot substrate, the plasma levitation requires a voltage difference between the liquid and the plate so that for most practical situations, the drop is attached to an electrode. However, capillary forces around this electrode are vanishingly small for very thin wires so that its mechanical effect on levitation can become negligible, and a usual free levitation process can be recovered.

¹B. Gottfried, C. Lee, and K. Bell, *Int. J. Heat Mass Transfer* **9**, 1167–1188 (1966).

²G. Zhang and G. Gogos, *J. Fluid Mech.* **222**, 543–563 (1991).

³A.-L. Bianco, C. Clanet, and D. Quéré, *Phys. Fluids* **15**, 1632–1637 (2003).

⁴K. Piroird, C. Clanet, and D. Quere, *Phys. Rev. E* **85**, 056311 (2012).

⁵F. Celestini and G. Kirstetter, *Soft Matter* **8**, 5992 (2012).

⁶S. Belostotskiy, T. Ouk, V. Donnelly, D. Economou, and N. Sadeghi, *J. Appl. Phys.* **107**, 053305 (2010).

⁷The full width at half maximum (FWHM) of a Voigt line profile, $\Delta\lambda_V$ is related to its Gaussian and Lorentzian (FWHM) components, $\Delta\lambda_G$ and $\Delta\lambda_L$, by the relation $\Delta\lambda_V^{1.4} = \Delta\lambda_L^{1.4} + \Delta\lambda_G^{1.4}$ in which $\Delta\lambda_L = \Delta\lambda_S + \Delta\lambda_P$ and $\Delta\lambda_G = (\Delta\lambda_D^2 + \Delta\lambda_I^2)^{1/2}$ [M. Ivkovic, S. Jovicevic, and N. Konjevic, *Spectrochim. Acta B* **59**, 591 (2004)].

⁸R. Konjevic and N. Konjevic, *Spectrochim. Acta B* **52**, 2077 (1997).

⁹M. A. Gigosos and V. Cardenoso, *J. Phys. B: At. Mol. Phys.* **29**, 4795 (1996).

¹⁰R. Redmer, “Physical properties of dense, low-temperature plasmas,” *Phys. Rep.* **282**(2-3), 35–157 (1997).

¹¹O. I. del Rio and A. W. Neumann, “Axisymmetric drop shape analysis: computational methods for the measurement of interfacial properties from the shape and dimensions of pendant and sessile drops,” *J. Colloid Interface Sci.* **196**(2), 136–147 (1997).

¹²See supplementary material at <http://dx.doi.org/10.1063/1.4926964> for details of the thermal model.

¹³Y. Raizer, *Gas Discharge Physics* (Springer Verlag, 1987).